## Table S1

| Antibody | Clone | Company |
|---|---|---|
| CD62L | MEL-14 | BD Biosciences |
| CD44 | IM7 | BD Biosciences |
| CD3ε | 2C11 | BD Biosciences |
| CD247 | MIH5 | BD Biosciences |
| CD11b | M1/70 | BD Biosciences |
| IFNγ | XMG1.2 | BD Biosciences |
| TNFα | MPG-XT22 | BD Biosciences |
| TCRβ | H57-597 | BD Biosciences |
| CD122 | TMβ1 | BD Biosciences |
| CD8α | 53-6.7 | ThermoFisher Scientific |
| Ki67 | SolA15 | ThermoFisher Scientific |
| FoxP3 | FJK-16s | ThermoFisher Scientific |
| NKG2D | CX5 | ThermoFisher Scientific |
| CD127/IL-7Rα | A7R34 | ThermoFisher Scientific |
| CD8β | 53-5.8 | Biolegend |
| Ly6C | HK1.4 | Biolegend |
| Ly6G | 1A8 | Biolegend |
| CD49b | DX5 | Biolegend |
| CD45.2 | 104 | Biolegend |
| CD4 | RM4-4 | Biolegend |
| CD4 | RM4-5 | Biolegend |
| CXCR3 | CXCR3-173 | Biolegend |
| CCR5 | HM-CCR5 | Biolegend |
| Granzyme B | GB11 | Invitrogen |

**Table S1. List of flow cytometry antibodies used for analysis of murine immune cell populations.**

## Table S2

| Cell Population | Flow Cytometry Gating Strategy |
|---|---|
| $CD8^+$ T Cells | Live/Singlet/$CD45.2^+$/$TCR\beta^+$/$CD8\alpha^+$ |
| $T_{CM}$ $CD8^+$ T Cells | Live/Singlet/$CD45.2^+$/$TCR\beta^+$/$CD8\alpha^+$/$CD44^{hi}$/$CD62L^{hi}$ |
| $T_{EM}$ $CD8^+$ T Cells | Live/Singlet/$CD45.2^+$/$TCR\beta^+$/$CD8\alpha^+$/$CD44^{hi}$/$CD62L^{lo}$/$CD127^{hi}$ |
| $T_{eff}$ $CD8^+$ T Cells | Live/Singlet/$CD45.2^+$/$TCR\beta^+$/$CD8\alpha^+$/$CD44^{hi}$/$CD62L^{lo}$/$CD127^{lo}$ |
| $CD4^+$ T Cells | Live/Singlet/$CD45.2^+$/$TCR\beta^+$/$CD4^+$/$FoxP3^-$ |
| $CD4^+$ $T_{reg}$ | Live/Singlet/$CD45.2^+$/$TCR\beta^+$/$CD4^+$/$FoxP3^+$ |
| NK Cells | Live/Singlet/$CD45.2^+$/$TCR\beta^-$/$CD49b^+$ |
| G-MDSC | Live/Singlet/$CD45.2^+$/$CD11b^+$/$F4/80^-$/$Ly6C^{lo}$/$Ly6G^{hi}$ |
| M-MDSC | Live/Singlet/$CD45.2^+$/$CD11b^+$/$F4/80^-$/Ly6Chi/$Ly6G^{lo}$ |
| Macrophages | Live/Singlet/$CD45.2^+$/$CD11b^+$/$F4/80^+$ |
| M1-like Macrophages | Live/Singlet/$CD45.2^+$/$CD11b^+$/$F4/80^+$/$CD38^+$ |
| M2-like Macrophages | Live/Singlet/$CD45.2^+$/$CD11b^+$/$F4/80^+$/$CD38^-$ |
| $CD45^+$ Cells | Live/Singlet/$CD45.2^+$ |
| $CD45^-$ Cells | Live/Singlet/$CD45.2^-$ |

**Table S2. Flow cytometry gating strategy used for identification of murine immune cell populations.**

**Table S3**

| | **0.3μg N-803 + 200μg αPD-L1** | **50μg N-809** | **100μg N-809** | **Fold increase of 50μg N-809 dose vs. N-803+αPD-L1** | **Fold increase of 100μg N-809 dose vs. N-803+αPD-L1** |
|---|---|---|---|---|---|
| N-803 dose | 0.3μg (15μg/kg) | 33μg | 66μg | 110 | 220 |
| αPD-L1 dose | 200μg (10mg/kg) | 50μg | 100μg | 0.25 | 0.5 |

**Table S3. N-809 vs. N-803+αPD-L1 dosing.** N-809 is a bifunctional molecule consisting of N-803 and αPD-L1. Table shows the doses of N-803 and αPD-L1 given with 0.3μg N-803+ 200μg αPD-L1, 50μg N-809, or 100μg N-809 administration and the fold increase in dose of N-809-delivered N-803 and αPD-L1 versus N-803+αPD-L1.

# Figure S1

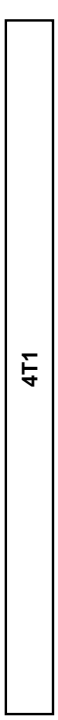


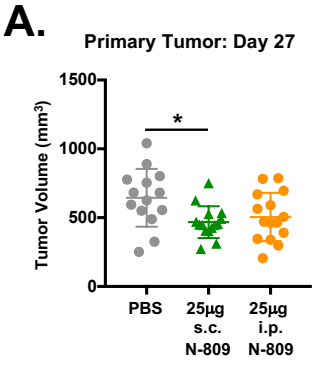


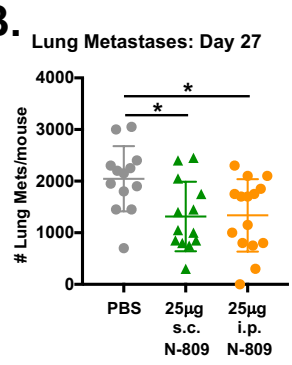


C.

**Lung Metastases**

| # Lung Mets / mouse | PBS n=13 | 25µg N-809 s.c. (n=13) | 25µg N-809 i.p. (n=15) |
|---|---|---|---|
| >2000 | 7/13 (54%) | 3/13 (23%) | 3/15 (20%) |
| ≤ 2000 | 6/13 (46%) | 10/13 (77%) | 12/15 (80%) |
| ≤ 1000 | 1/13 (7%) | 6/13 (46%) | 6/15 (40%) |
| ≤ 500 | 0/13 (0%) | 1/13 (7%) | 2/15 (13%) |
| ≤ 100 | 0/13 (0%) | 0/13 (0%) | 1/15 (7%) |
| ≤ 10 | 0/13 (0%) | 0/13 (0%) | 1/15 (7%) |
| Mean | 2046 | 1315 | 1337 |
| % Reduction vs. PBS | | 36% | 35% |

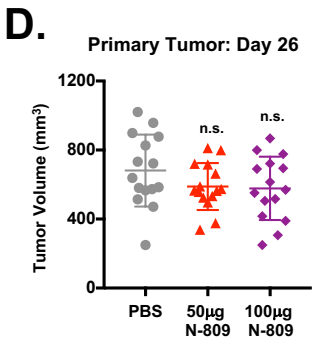


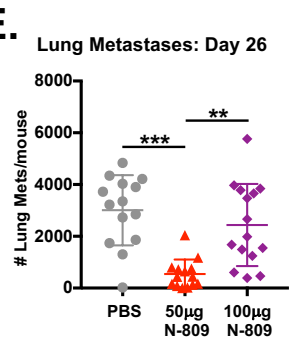


F.

**Lung Metastases**

| # Lung Mets / Mouse | PBS (n=14) | 50µg N-809 (n=14) | 100µg N-809 (n=15) |
|---|---|---|---|
| ≥ 4000 | 4/14 (29%) | 0/14 (0%) | 1/15 (7%) |
| ≤ 4000 | 10/14 (71%) | 14/14 (100%) | 14/15 (93%) |
| ≤ 2000 | 4/14 (29%) | 13/14 (93%) | 8/15 (53%) |
| ≤ 1000 | 1/14 (7%) | 12/14 (86%) | 3/15 (20%) |
| ≤ 500 | 1/14 (7%) | 8/14 (57%) | 2/15 (13%) |
| ≤ 100 | 1/14 (7%) | 3/14 (21%) | 0/15 (0%) |
| 0 | 0/14 (0%) | 1/14 (7%) | 0/15 (0%) |
| Mean | 3009 | 541 | 2439 |
| % Reduction vs. PBS | | 82% | 19% |


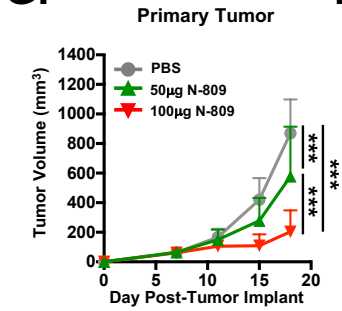


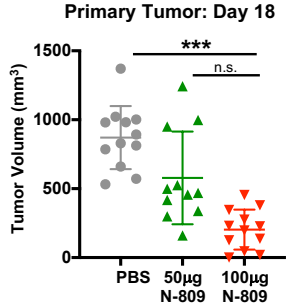


| | PBS | 50µg N-809 | 100µg N-809 |
|---|---|---|---|
| # Cures | 0/13 | 0/13 | 1/13 |
| % Cure | 0% | 0% | 8% |

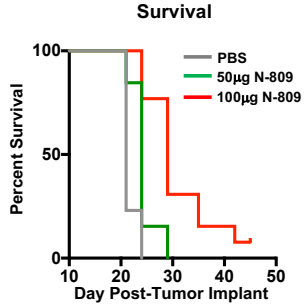


| | PBS | 50µg N-809 | 100µg N-809 |
|---|---|---|---|
| Median OS (d) | 21 | 24 | 29 |
| Mantel-Cox | | | |
| vs. PBS | | p=0.002 | p<0.0001 |
| vs. 100µg N-809 | p<0.0001 | p=0.001 | |

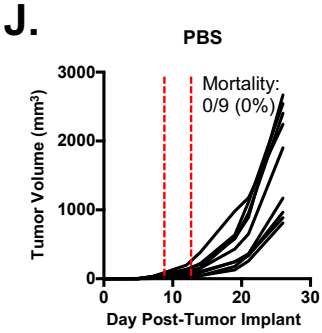


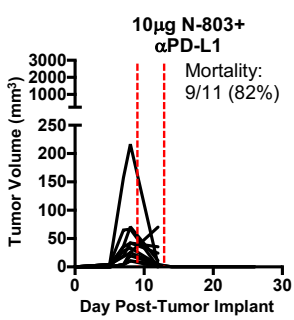


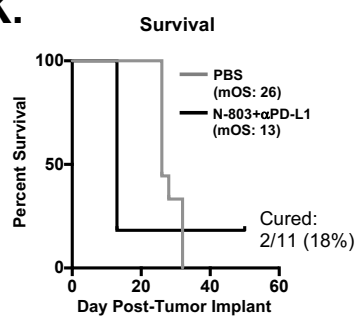

**Figure S1.**
**(A-C) N-809 promotes similar anti-tumor efficacy in 4T1 tumor-bearing mice when administered i.p. or s.c.** 4T1 tumors were implanted as in Figure 1 and mice were treated at days 9 and 13 with 25μg N-809 i.p. or s.c. Graphs of tumor volumes **(A)** and number of lung metastases in individual mice at day 27 post-tumor implant **(B)** show mean±SD. **(C)** Table denotes the distribution of number of lung metastases and % reduction in mean vs. PBS. Data are from one independent experiment, n=13-15 mice.

**(D-F) 50μg N-809 reduces lung metastasis in 4T1 tumor-bearing mice greater than 100μg N-809.** 4T1 tumors were implanted as in Figure 1 and mice were treated at days 9 and 13 with 50μg or 100μg N-809 (s.c.). Graphs of tumor volumes **(D)** and number of lung metastases in individual mice at day 26 post-tumor implant **(E)** show mean±SD. **(F)** Table denotes the distribution of number of lung metastases and % reduction in mean vs. PBS. Data are from one independent experiment, n=13-15 mice.

**(G-I)** MC38 tumors were implanted as in Figure 1 and mice were treated at days 8 and 12 with 50μg N-809 (s.c.) or 100μg N-809 (s.c.). Data from PBS and 100μg N-809 are the same as shown in Figure 2F-H. Primary tumor growth curves **(G)** and tumor volumes of individual mice at day 18 (inset: % cured mice) **(H)** show mean±SD. **(I)** Survival curves (inset: mOS) show % survival. Data are representative of two independent experiments, n=13 mice.

**(J-K) 10μg N-803 (1/6 IL-15 equimolar dose vs. 100μg N-809) induces ~80% mortality in MC38 tumor-bearing mice.** MC38 tumors were implanted as in Figure 1 and mice were treated at days 9 and 13 with 10μg N-803+200μg αPD-L1. Red dashed lines denote treatments. Primary tumor growth curves of individual mice (inset: % mortality post-treatment) shown in **(J)** and survival curves (inset: mOS, % cures) show % survival **(K)**. Data are from one experiment, n=10 mice.

**Figure S2**

**A.** 4T1 Tumor-Bearing Mice: Body Weight

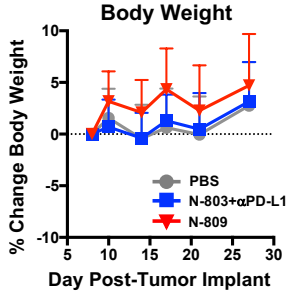


**B.** 4T1 Tumor-Bearing Mice: Histopathology

| | DAY 15 | | | |
|---|---|---|---|---|
| | **PBS (n=3)** | **N-803+ αPD-L1 (n=3)** | **50μg N-809 (n=3)** | **Naïve (n=1)** |
| **Lung** | 3/3 Chronic pneumonitis: 1/3 Mild 1/3 Moderate 1/3 Severe | 3/3 Chronic pneumonitis: 1/3 Mild 2/3 Severe | 3/3 Chronic pneumonitis: 3/3 Severe | 1/1 Chronic pneumonitis: 1/1 Mild |
| **Brain, intestine, heart, kidney, and liver were all normal.** | | | | |

**C.** MC38 Tumor-Bearing Mice: Body Weight

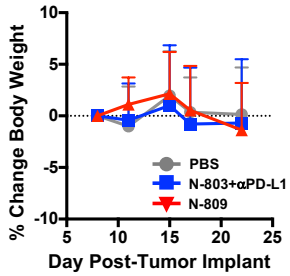


**D.** MC38 Tumor-Bearing Mice: Histopathology

| | DAY 15 | | | | |
|---|---|---|---|---|---|
| | **PBS (n=8)** | **N-803+ αPD-L1 (n=8)** | **50μg N-809 (n=8)** | **100μg N-809 (n=8)** | **Naïve (n=6)** |
| **Brain** | 8/8 Normal | 8/8 Normal | 5/5 Normal | 8/8 Normal | 6/6 Normal |
| **Intestine** | 6/8 Normal, 2/8 Small bowel epithelial necrosis | 8/8 Normal | 5/5 Normal | 8/8 Normal, 1/8 Small bowel epithelial necrosis | 6/6 Normal |
| **Heart** | 8/8 Normal | 8/8 Normal | 5/5 Normal | 7/8 Normal, 1/8 Chronic active myocarditits | 5/6 Normal, 1/6 Chronic active myocarditits |
| **Kidney** | 8/8 Normal | 8/8 Normal | 5/5 Perinephritis | 8/8 Perinephritis | 6/6 Normal |
| **Liver** | 8/8 Normal | 4/8 Normal, 4/8 Chronic hepatitis: 4/8 Mild | 5/5 Chronic hepatitis: 2/5 Mild 3/5 Moderate | 8/8 Chronic hepatitis: 1/8 Mild 7/8 Moderate | 6/6 Normal |
| **Lung** | 1/8 Normal, 7/8 Chronic pneumonitis: 3/8 Mild 4/8 Moderate | 1/8 Normal, 7/8 Chronic pneumonitis: 6/8 Mild 1/8 Moderate | 5/5 Chronic pneumonitis: 4/5 Moderate 1/5 Severe | 8/8 Chronic pneumonitis: 3/8 Mild 2/8 Moderate 3/8 Severe | 3/6 Normal, 3/6 Chronic pneumonitis: 3/6 Mild |

| | DAY 23 | | | | |
|---|---|---|---|---|---|
| | **PBS (n=5)** | **N-803+ αPD-L1 (n=5)** | **50μg N-809 (n=3)** | **100μg N-809 (n=4)** | **Naïve (n=6)** |
| **Brain** | 5/5 Normal | 5/5 Normal | 3/3 Normal | 4/4 Normal | 6/6 Normal |
| **Intestine** | 4/5 Normal, 1/5 Chronic duodenitis | 4/5 Normal, 1/5 Small bowel epithelial necrosis | 2/3 Normal, 1/3 Small bowel epithelial necrosis | 3/4 Normal, 1/4 Small bowel epithelial necrosis | 6/6 Normal |
| **Heart** | 5/5 Normal | 5/5 Normal | 3/3 Normal | 4/4 Normal | 5/6 Normal, 1/6 Chronic active myocarditits |
| **Kidney** | 5/5 Normal | 5/5 Normal | 3/3 Normal | 4/4 Normal | 6/6 Normal |
| **Liver** | 5/5 Normal | 5/5 Normal | 3/3 Normal | 4/4 Normal | 6/6 Normal |
| **Lung** | 2/5 Normal, 3/5 Chronic pneumonitis: 3/5 Mild | 4/5 Normal, 1/5 Chronic pneumonitis: 1/5 Mild | 2/3 Normal, 1/3 Chronic pneumonitis: 1/3 Mild | 1/4 Normal, 3/4 Chronic pneumonitis: 2/4 Mild 1/4 Moderate | 3/6 Normal, 3/6 Chronic pneumonitis: 3/6 Mild |

**Figure S2. N-809 does not induce toxicity in 4T1 tumor-bearing mice but does induce transient, dose-dependent, non-lethal toxicity in MC38 tumor-bearing mice.** 4T1 tumors **(A-B)** or MC38 tumors **(C-D)** were implanted as in Figure 2 and mice were treated at days 9 and 13 with 0.3μg N-803 (s.c.)+200μg αPD-L1 (i.p.), 50μg N-809 (s.c.), or 100μg N-809 (s.c.). **(A,C)** Body weight was determined 1-2 times per week for the duration of the experiment. Data are from 1 experiment, n=8-15 mice/group. **(B,D)** Mice were sacrificed 2 or 10 days after the last treatment. Tables show histopathology as determined by H&E staining of the listed organs. Naïve listed in **(D)** is the same cohort of mice for days 15 and 23. Data are combined from 1-2 experiments, n=3-5 mice/group per experiment.

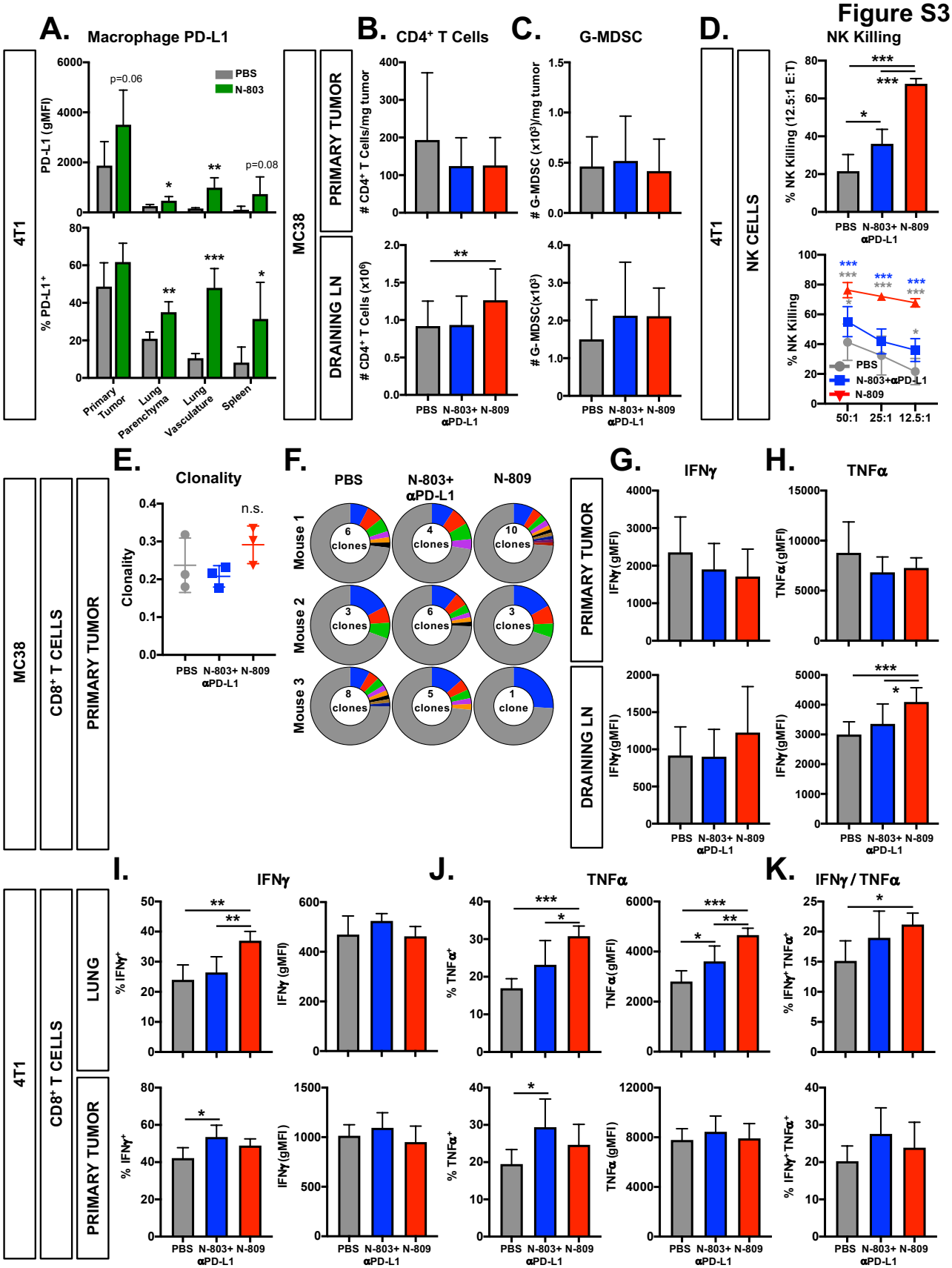
Figure S3
A.
Macrophage PD-L1
4T1
PD-L1 (gMFI)
% PD-L1+
PBS
N-803
p=0.06
p=0.08
Primary Tumor
Lung Parenchyma
Lung Vasculature
Spleen
MC38
PRIMARY TUMOR
DRAINING LN
B.
CD4+ T Cells
# CD4+ T Cells/mg tumor
# CD4+ T Cells (x10^6)
C.
G-MDSC
# G-MDSC (x10^3)/mg tumor
# G-MDSC(x10^3)
D.
4T1
NK CELLS
NK Killing
% NK Killing (12.5:1 E:T)
% NK Killing
PBS
N-803+αPD-L1
N-809
50:1
25:1
12.5:1
PBS N-803+ N-809 αPD-L1
E.
Clonality
Clonality
n.s.
F.
PBS
N-803+ αPD-L1
N-809
Mouse 1
Mouse 2
Mouse 3
6 clones
4 clones
10 clones
3 clones
6 clones
3 clones
8 clones
5 clones
1 clone
MC38
CD8+ T CELLS
PRIMARY TUMOR
G.
IFNγ
IFNγ(gMFI)
H.
TNFα
TNFα(gMFI)
I.
IFNγ
% IFNγ+
IFNγ (gMFI)
J.
TNFα
% TNFα+
TNFα (gMFI)
K.
IFNγ / TNFα
% IFNγ+ TNFα+
4T1
CD8+ T CELLS
LUNG
PRIMARY TUMOR

**Figure S3.**
**(A) N-803 increases PD-L1 expression on macrophages in 4T1 tumor-bearing mice.** 4T1 tumors were implanted and mice were treated on days 12 and 16 with 1μg N-803 s.c. PD-L1 expression was detected by flow cytometry on macrophages 24 hours post-treatment. Data are from one experiment, n=5 mice/group.

**(B-C) N-809 does not greatly alter number of CD4⁺ T cells or G-MDSC in the tumor and draining LN of MC38 tumor-bearing mice.** MC38 tumors were implanted and mice were treated as in Figure 4. The number of CD4⁺ T cells **(B)** and G-MDSC **(C)** were examined by flow cytometry in the primary tumor (top) and draining LN (bottom) 48 hours after treatment. Data are combined from 2-3 independent experiments, n=5 mice/group per experiment.

**(D) N-809 enhances NK killing in 4T1 tumor-bearing mice.** 4T1 tumors were implanted and treated as in Figure 2. Purified splenic NK cells were co-cultured with $^{111}$In-labeled Yac-1 target cells at the designated effector-to-target (E:T) ratios for 18 hours. $^{111}$In release was measured to determine cytotoxic function. Data are from one independent experiment, n=5 mice/group.

**(E-F) N-809 does not alter clonality of CD8⁺ T cells in the TME of MC38 tumor-bearing mice.** MC38 tumors were implanted and mice were treated as in Figure 4. At day 17 post-tumor implant, intratumoral CD8⁺ T cells were isolated and subjected to TCRβ sequencing. **(E)** Graph shows clonality of functional TCRβ chains detected in intratumoral CD8⁺ T cells. **(F)** Pie charts show number of TCRβ clones that comprise the top ~25% of detected sequences. Colors indicate the prevalence of each TCRβ clone and are not representative of the same shared TCRβ clone in independent samples. Data are from one experiment, n=3 mice/group.

**(G-H) Effect of N-809 on CD8⁺ T cell cytokine production in the tumor and draining LN of MC38 tumor-bearing mice.** MC38 tumors were implanted and mice were treated as in Figure 4. Two days after treatment, immune cells from the primary tumor (top) or draining LN (bottom) were stimulated with 1μg/ml αCD3+1μg/ml αCD28 for 4 hours. Graphs show IFNγ **(G)** or TNFα **(H)** production by CD8⁺ T cells as geometric mean fluorescence intensity (gMFI). Data combined from 2-3 independent experiments, n=5 mice/group per experiment.

**(I-K) N-809 increases CD8⁺ T cell function in the lung of 4T1 tumor-bearing mice.** 4T1 tumors were implanted and treated as in Figure 2. Two days after treatment, immune cells from the lung parenchyma (top) or primary tumor (bottom) were stimulated with 1μg/ml αCD3+1μg/ml αCD28 for 4 hours. Graphs show frequency of total IFNγ⁺ or IFNγ production **(I)**, frequency of total TNFα⁺ or TNFα production **(J)**, and IFNγ/TNFα-double producing **(K)** CD44$^{hi}$ CD8⁺ T cells as determined by flow cytometry. Data from one experiment, n=5 mice/group.

All graphs show mean±SD.

**Figure S4**

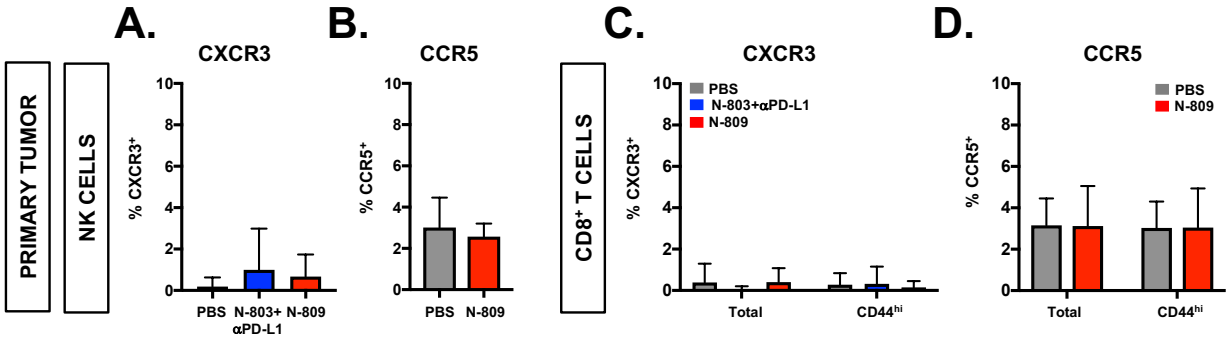


**Figure S4. Effect of N-809 on chemokine receptor expression on NK cells and CD8⁺ T cells in the tumor.** MC38 tumors were implanted and mice treated as in Figure 2. NK cells **(A-B)** and CD8⁺ T cells **(C-D)** were examined by flow cytometry in the primary tumor. Graphs show CXCR3⁺ **(A)** or CCR5⁺ **(B**) NK cells and CXCR3⁺ **(C)** or CCR5⁺ **(D**) total or CD44$^{hi}$ CD8⁺ T cells. Data are combined from 1-2 independent experiments, n=5 mice/group per experiment.